

## Multimodal Image-Guided Enzyme/Prodrug Cancer Therapy

Cong Li, Paul T. Winnard, Jr., Tomoyo Takagi, Dmitri Artemov, and Zaver M. Bhujwala\*

JHU ICMIC Program, The Russell H. Morgan Department of Radiology and Radiological Science,  
The Johns Hopkins University School of Medicine, Baltimore, Maryland 21205

Received August 25, 2006; E-mail: zaver@mri.jhu.edu

Strategies for optimizing enzyme/prodrug therapy are an active area of research in cancer treatment.<sup>1</sup> In these strategies, a tumor-targeted drug-activating enzyme is delivered. After the clearance of unbound enzyme from normal tissues, a nontoxic prodrug, which is a substrate of the enzyme, is administered. The prodrug is converted to the anticancer drug by the enzyme in the tumor, while normal tissues lacking the enzyme are spared from toxicity. Conversion of the prodrug by residual enzyme in normal tissues may lead to toxicity if the prodrug is injected too early, and low tumor concentrations of the enzyme due to clearance or proteolytic degradation may result in diminishing concentration of active drug in the tumor if the prodrug is given too late.<sup>2</sup> Determining the optimal time-window for prodrug injection is therefore of utmost importance for success of these strategies. Imaging the delivery of a drug-activating enzyme would be ideal to optimize the timing of prodrug delivery. Here we report the first drug-activating enzyme functionalized with multimodal imaging reporters to provide image-guided delivery of a prodrug.

Cytosine deaminase converts the nontoxic prodrug 5-fluorocytosine (5FC) to the anti-cancer drug 5-fluorouracil (5FU).<sup>3</sup> 5FU and its metabolites, such as 5-fluorodeoxyuridine-5'-monophosphate (5-FdUMP), can ultimately lead to the inhibition of DNA synthesis.<sup>4</sup> In this work, bacterial cytosine deaminase (bCD) was chosen as the therapeutic enzyme due to its high enzymatic stability.<sup>5</sup> Poly-L-lysine (PLL) ( $M_r = 5.6$  kDa) was selected as a carrier of the imaging reporters because it is biodegradable and its extended random coil conformation may facilitate the extravasation of the conjugate into the tumor interstitium.<sup>6</sup> PLL was functionalized with  $Gd^{3+}$ -DOTA and rhodamine to dynamically monitor in vivo distribution of bCD by either MRI or optical imaging. Rhodamine can also track the enzyme in excised tissue. Biotins grafted on PLL allow the rapid clearance of the bCD-PLL conjugate from circulation by using avidin chase without affecting the extravasated material.<sup>7</sup> Additionally, the conversion of 5FC to 5FU can be detected noninvasively in vivo with <sup>19</sup>F MR spectroscopy.<sup>8</sup> The resulting bCD-PLL conjugate ( $M_w > 300$  kDa) is expected to extravasate into the tumor interstitium but not normal tissues due to the high permeability of tumor vasculature.<sup>9</sup>

The synthesis of the bCD-PLL **1** is outlined in Scheme 1. Briefly, treatment of NHS esters of rhodamine, biotin, and DOTA with PLL, respectively, gave **3**. After complexation with  $Gd^{3+}$ , a maleimide moiety was introduced to give **5**. The molar equivalent ratios of rhodamine, biotin, and  $Gd^{3+}$ -DOTA to PLL in **4** were determined as 0.8:1, 3:1, and 14:1, respectively (see Supporting Information (SI)). A bCD cDNA vector<sup>3b</sup> was used for producing the bCD protein in large quantities from transformed *Escherichia coli* cultures. A sulfhydryl group was specifically introduced to the N-terminal of the bCD protein at pH 7.0 in two steps. The coupling between **5** and **7** gave bCD-PLL **1**. The ratio of the bCD hexamer to PLL in **1** was determined as 1:1.1 by measuring the absorbance of bCD subunits ( $\epsilon_{279} = 76\,000\text{ M}^{-1}\text{ cm}^{-1}$ ) and rhodamine ( $\epsilon_{572} =$

**Scheme 1.** Synthetic Procedure for bCD-PLL **1** Conjugate

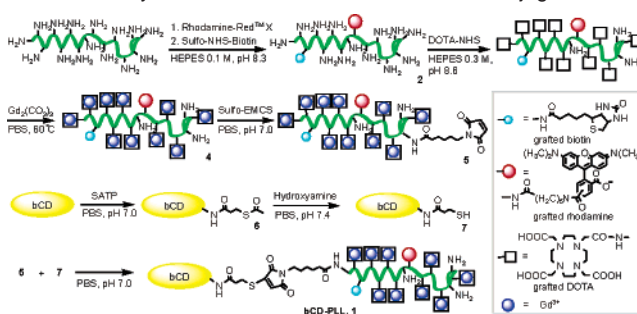


**Table 1.** Kinetic Values of bCD and bCD-PLL **1**<sup>a</sup>

	Cytosine (5-Fluorocytosine)				
	$K_m$ (mM)	$k_{cat}^c$ (s <sup>-1</sup> )	$k_{cat}/K_m$ (mM <sup>-1</sup> s <sup>-1</sup> )	specific activity ( $\mu\text{mol}\cdot\text{min}^{-1}\text{ mg}^{-1}$ )	R.S. <sup>f</sup>
bCD <sup>b</sup>	0.19 (3.9)	185 (71)	973 (18)	144 <sup>d</sup> (58) <sup>e</sup>	0.018
<b>1</b> <sup>b</sup>	0.16 (3.7)	148 (74)	925 (20)	121 <sup>d</sup> (61) <sup>e</sup>	0.021

<sup>a</sup> Determined in 50 mM Tris buffer, pH 7.5 at 25 °C. <sup>b</sup> Protein concentration was measured from the absorbance of bCD monomer ( $\epsilon_{279} = 76\text{ mM}^{-1}\text{ cm}^{-1}$ ). <sup>c</sup>  $k_{cat}$  values were calculated using the equation  $k_{cat} = V_{max}/[E]$ . Assays are described in SI. <sup>d</sup> Determined in 0.5 mM cytosine. <sup>e</sup> Determined in 9.6 mM 5FC. <sup>f</sup> Relative specificities (R.S.) were calculated using the equation  $[k_{cat}/K_m(5FC)]/[k_{cat}/K_m(\text{cytosine}) + k_{cat}/K_m(5FC)]$ .

120 000  $\text{M}^{-1}\text{ cm}^{-1}$ ). The average  $M_w$  values of bCD-PLL and bCD were determined as 345 and 302 kDa by size-exclusion chromatography (see SI). Effluent peaks of bCD-PLL with identical  $V_e/V_o$  values ( $V_e =$  elution volume;  $V_o =$  void volume) were observed by monitoring the absorbance at 279 (bCD) and 572 nm (rhodamine) in separate experiments, which validated bCD-PLL as a covalent complex (Figure S2). A narrow molecular size distribution of bCD-PLL was detected by dynamic light scattering (DLS) with an average hydrodynamic radius of 9.4 nm (Figure S3), which is beneficial for its extravasation into the tumor.<sup>9</sup> The conjugation of rhodamine to PLL resulted in a slight red shift of the emission spectrum centered at 590 nm (Figure S5). The water proton longitudinal relaxivities,  $r_{1p}$ , of compound **4** and bCD-PLL at 4.7 T, 25 °C, were measured as 5.8 and 8.6  $\text{mM}^{-1}\text{ s}^{-1}/Gd^{3+}$  ion at pH 7.4 (Figure S6). In comparison with the clinically used MRI contrast agents, such as  $Gd^{3+}$ -DOTA ( $r_{1p} = 4.3\text{ mM}^{-1}\text{ s}^{-1}$ ), the substantially increased  $r_{1p}$  of bCD-PLL can be attributed to the augmentation of the rotational correlation lifetime  $\tau_R$  of  $Gd^{3+}$  chelates upon attachment to the bulky bCD hexamer.<sup>10</sup>

The kinetic values of bCD-PLL to the substrates cytosine and 5-fluorocytosine (5FC) were assayed by monitoring the absorbance variation of cytosine ( $\Delta\epsilon_{286} = -0.68\text{ mM}^{-1}\text{ cm}^{-1}$ ) and 5FC ( $\Delta\epsilon_{297} = -0.41\text{ mM}^{-1}\text{ cm}^{-1}$ ).<sup>11</sup> The data were transformed into linear Woolf plots,<sup>12</sup> from which  $K_m$  and  $k_{cat}$  were obtained (Table 1). The bCD-PLL exhibited similar  $K_m$  values to both substrates as bCD, indicating that conjugation of bCD to PLL did not compro-

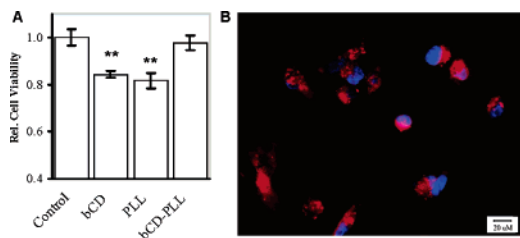


**Figure 1.** (A) In vitro cytotoxicity of bCD, PLL, and bCD-PLL in a human breast cancer cell line, MDA-MB-231, acquired from an MTT assay at a dose of  $4.3 \mu\text{M}$  that will be used for in vivo studies. Standard deviations are shown with error bars ( $n = 4$ ); \*\* indicates statistical significance at levels of  $p < 0.01$  for the PLL or bCD versus control. (B) Internalization of bCD-PLL within MDA-MB-231 cells after treatment with bCD-PLL ( $100 \text{ ng/mL}$ ) for 30 min. Rhodamine fluorescence is shown in red, and nuclei counterstained with DAPI are displayed in blue.

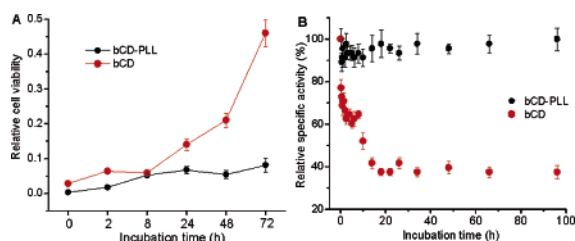


**Figure 2.** (A) Relative cell viability of MDA-MB-231 cells after incubation with therapeutic enzyme ( $0.13 \mu\text{M}$ ) for 0–72 h following additional 5 day treatment with prodrug 5FC ( $1.5 \text{ mg/mL}$ ). (B) Dynamic enzymatic activity of bCD and bCD-PLL in fresh mouse serum at  $37^\circ\text{C}$ . Enzymatic activity was measured in  $0.5 \text{ mM}$  cytosine, Tris-HCl ( $50 \text{ mM}$ ), pH 7.5,  $25^\circ\text{C}$ . Standard deviations are shown with error bars ( $n = 4$ ).

mise its enzymatic activity. In fact, compared to bCD, bCD-PLL demonstrated a slightly increased preference to 5FC relative to cytosine with higher  $k_{\text{cat}}$  and  $k_{\text{cat}}/K_{\text{m}}$  values. The relative enzymatic specificity<sup>11</sup> of bCD-PLL to 5FC was determined to be 0.021, while the value was 0.018 for bCD.

The cytotoxicity of bCD-PLL in a human breast cancer cell line, MDA-MB-231, was studied using an MTT assay.<sup>13</sup> The concentrations used were derived from estimates to generate  $165 \text{ mg/kg}$  of 5FU typically used to treat experimental tumors in vivo.<sup>14</sup> Both PLL and bCD exhibited moderate toxicity with a relative cell viability of 84 and 82% after 5 days incubation (Figure 1A), whereas no obvious cytotoxicity was detected for bCD-PLL. Fluorescence microscopy showed that bCD-PLL can be internalized by MDA-MB-231 cells efficiently even after a 30 min treatment (Figure 1B). The PLL moiety may facilitate the cell uptake of bCD-PLL through polycation-mediated endocytosis.<sup>15</sup>

The enzymatic stability of bCD-PLL was tested on cultured tumor cells. Briefly, MDA-MB-231 cells were incubated with various concentrations ( $0.13$ – $4.3 \mu\text{M}$ ) of bCD-PLL for 0, 2, 8, 24, 48, and 72 h before the addition of 5FC. At the end of 5 days of prodrug treatment, the relative cell viabilities were evaluated (Figure S8). The bCD-PLL remained capable of converting sufficient 5FC to 5FU to cause 90% cell death at all concentrations ( $0.13$ – $4.3 \mu\text{M}$ ) and incubation periods (0–72 h). However, bCD exhibited enzymatic stability lower than that of bCD-PLL as indicated by the increased cell viability observed at the longer time points with low bCD concentrations (Figure 2A). The enzymatic stability of bCD-PLL was further studied in fresh mouse serum at  $37^\circ\text{C}$  (Figure 2B). Significantly, while bCD lost about 60% of its cytosine metabolizing capability in the initial 20 h incubation,

the activity of bCD-PLL remained nearly unaffected throughout the remaining 4 day incubation. We hypothesize that, like poly(ethylene glycol) (PEG),<sup>16</sup> the attached polylysine in bCD-PLL may produce a steric exclusion space that prevents the proteolysis of bCD by proteases such as cathepsins and matrix metalloproteinases (MMPs) that are overexpressed in highly invasive cancer cell lines, such as MDA-MB-231.<sup>17</sup>

In summary, we have developed a novel cancer therapeutic enzyme labeled with multimodal imaging reporters demonstrating high relaxivity, low cytotoxicity, improved enzymatic specificity to prodrug, efficient cell uptake, and high enzymatic stability in serum as well as in breast cancer cell culture. This conjugate is the first prototype for noninvasive image-guided enzyme/prodrug cancer therapy. In vivo studies of this conjugate in tumor xenograft models are currently underway.

**Acknowledgment.** This work was supported by NIH P50 CA103175 (JHU ICMIC Program). We thank Dr. Barry Stoddard of the Fred Hutchinson Cancer Research Center for providing the pET-bCD expression vector. We thank Dr. Michal Neeman, Dr. Venu Raman, and Dr. Peter Senter for helpful discussions. We thank Dr. Maria Mikhaylova for her assistance with the DLS and ICP-AES studies. We gratefully acknowledge the support of Dr. Jonathan S. Lewin.

**Supporting Information Available:** Synthesis and characterization of the bCD-PLL conjugate, kinetic studies, in vitro cytotoxicity and cell uptake studies, enzymatic stability studies in serum, and cell culture. This material is available free of charge via the Internet at <http://pubs.acs.org>.

## References

- (1) (a) Xu, G.; McLeod, H. L. *Clin. Cancer Res.* **2001**, *7*, 3314–3324. (b) Bagshawe, K. D.; Sharma, S. K.; Burke, P. J.; Melton, R. D.; Knox, R. *J. Curr. Opin. Immunol.* **1999**, *11*, 579–583.
- (2) Niculescu-Duvaz, I.; Springer, C. J. *Adv. Drug Delivery Rev.* **1997**, *2*, 151–172.
- (3) (a) Ireton, G. C.; McDermott, G.; Black, M. E.; Stoddard, B. L. *J. Mol. Biol.* **2002**, *315*, 687–697. (b) Ireton, G. C.; Black, M. E.; Stoddard, B. L. *Acta Crystallogr., Sect. D* **2001**, *57*, 1643–1645.
- (4) Mahan, S. D.; Ireton, G. C.; Stoddard, B. L.; Black, M. E. *Biochemistry* **2004**, *43*, 8957–8964.
- (5) Mahan, S. D.; Ireton, G. C.; Knoeber, C.; Stoddard, B. L.; Black, M. *Protein Eng. Des. Sel.* **2004**, *17*, 625–633.
- (6) Uzgiris, E. E. *Invest. Radiol.* **2001**, *39*, 131–137.
- (7) Dafni, H.; Gilead, A.; Nevo, N.; Eilam, R.; Harmelin, A.; Neeman, M. *Magn. Reson. Med.* **2003**, *50*, 904–914.
- (8) Aboagye, E. O.; Artemov, D.; Senter, P. D.; Bhujwala, Z. M. *Cancer Res.* **1998**, *58*, 4075–4078.
- (9) (a) Jain, R. K. *J. Controlled Release* **2001**, *74*, 7–25. (b) Yuan, F.; Dellian, M.; Fukumura, D.; Leunig, M.; Berk, D. A.; Torchilin, V. P.; Jain, R. K. *Cancer Res.* **1995**, *55*, 3752–3756.
- (10) Aime, S.; Botta, M.; Fasano, M.; Terreno, E. *Chem. Soc. Rev.* **1998**, *27*, 19–29.
- (11) (a) Ippata, P. L.; Cercignani, G. *Methods Enzymol.* **1978**, *51*, 395–400. (b) Hayden, M. S.; Linsley, P. S.; Wallace, A. R.; Marquardt, H.; Kerr, D. E. *Protein Expr. Purif.* **1998**, *12*, 173–184.
- (12) Cornish-Bowden, A. *Fundamentals of Enzyme Kinetics*; Portland Press Ltd: London, 1995; pp 30–37.
- (13) For detailed information about MTT assay, see: Li, C.; Greenwood, T. R.; Bhujwala, Z. M.; Glunde, K. *Org. Lett.* **2006**, *8*, 3623–3626.
- (14) Aboagye, E. O.; Bhujwala, Z. M.; Shungu, D. C.; Glickson, J. D. *Cancer Res.* **1998**, *58*, 1063–1067.
- (15) Hong, S.; Leroueil, P. R.; Janus, E. K.; Peters, J. L.; Kober, M. M.; Islam, M. T.; Orr, B. G.; Baker, J. R., Jr.; Banaszak Holl, M. M. *Bioconjugate Chem.* **2006**, *17*, 728–734.
- (16) (a) Harris, J. M.; Chess, R. B. *Nat. Rev. Drug Discovery* **2003**, *2*, 214–221. (b) Veronese, F. M.; Harris, J. M. *Adv. Drug Delivery Syst.* **2002**, *54* (4), whole issue.
- (17) (a) Ishibashi, O.; Mori, Y.; Kurokawa, T.; Kumegawa, M. *Cancer Biochem. Biophys.* **1999**, *17*, 69–78. (b) Munoz-Najar, U. M.; Neurath, K. M.; Vumbaca, F.; Claffey, K. P. *Oncogene* **2006**, *25*, 2379–2392.

JA066199I